JOURNAL OF GEOPHYSICAL RESEARCH: SPACE PHYSICS, VOL. 118, 1180–1189, doi:10.1002/jgra.50116, 2013

Direct observations of the role of convection electric field in the formation of a polar tongue of ionization from storm enhanced density

E. G. Thomas,[1] J. B. H. Baker,[1] J. M. Ruohoniemi,[1] L. B. N. Clausen,[1,2] A. J. Coster,[3] J. C. Foster,[3] and P. J. Erickson[3]

Received 12 October 2012; revised 8 January 2013; accepted 9 January 2013; published 1 March 2013.

[1] We examine the relationship of convection electric fields to the formation of a polar cap tongue of ionization (TOI) from midlatitude plumes of storm enhanced density (SED). Observations from the geomagnetic storm on 26–27 September 2011 are presented for two distinct SED events. During an hour-long period of geomagnetic activity driven by a coronal mass ejection, a channel of high-density *F* region plasma was transported from the dayside subauroral ionosphere and into the polar cap by enhanced convection electric fields extending to middle latitudes. This TOI feature was associated with enhanced HF backscatter, indicating that it was the seat of active formation of small-scale irregularities. After the solar wind interplanetary magnetic field conditions quieted and the dayside convection electric fields retreated to higher latitudes, an SED plume was observed extending to, but not entering, the dayside cusp region. This prominent feature in the distribution of total electron content (TEC) persisted for several hours and elongated in magnetic local time with the rotation of the Earth. No ionospheric scatter from SuperDARN radars was observed within this SED region. The source mechanism (enhanced electric fields) previously drawing the plasma from midlatitudes and into the polar cap as a TOI was no longer active, resulting in a fossil feature. We thus demonstrate the controlling role exercised by the convection electric field in generating a TOI from midlatitude SED.

Citation: Thomas, E. G., J. B. H. Baker, J. M. Ruohoniemi, L. B. N. Clausen, A. J. Coster, J. C. Foster, and P. J. Erickson (2013), Direct observations of the role of convection electric field in the formation of a polar tongue of ionization from storm enhanced density, *J. Geophys. Res. Space Physics*, *118*, 1180–1189, doi:10.1002/jgra.50116.

1. Introduction

[2] The plasma of Earth's ionosphere at high latitudes is subject to redistribution by strong electric fields of magnetospheric origin. At *F* region altitudes centered on 200–400 km, both ions and electrons drift with a nearly horizontal velocity given by $\mathbf{v} = \mathbf{E} \times \mathbf{B}/B^2$, where $\mathbf{E}$ is the ionospheric electric field and $\mathbf{B}$ is the geomagnetic field. The large-scale motion of the plasma most often conforms to a two-cell pattern, with antisunward flow from the dayside across the polar cap to the nightside and return flow at auroral latitudes in the dawn and dusk sectors [*Heppner and Maynard*, 1987; *Ruohoniemi and Greenwald*, 1996].

[3] A tongue of ionization (TOI) is a channel of high-density *F* region plasma transported from the dayside midlatitude ionosphere through the cusp and into the polar cap by enhanced convection electric fields [*Sato*, 1959; *Sato and Rourke*, 1964; *Knudsen*, 1974]. Storm enhanced density (SED) is a plume of ionization in the dusk sector that is carried sunward and poleward by the low-latitude edge of the subauroral polarization stream (SAPS) [*Foster et al.*, 2004; *Foster and Burke*, 2002; *Foster and Vo*, 2002] during major disturbances. Both features are characterized by enhanced densities, an elevated *F* peak altitude, and low electron and ion temperatures [*Foster*, 1993]. Phenomenologically, SED is primarily a feature of the postnoon sector at middle latitudes with significant elongation in longitude while TOI is more elongated in a latitudinal sense from middle to polar latitudes in the noon sector.

[4] The source of plasma for the TOI has been a particular focus of study. *Foster et al.* [2005] presented a multi-instrument analysis of the polar TOI during a large geomagnetic storm and suggested that the dayside source of the TOI was an SED plume transported from subauroral latitudes in the dusk sector by SAPS disturbance electric fields. The plume of enhanced total electron content (TEC) was seen to closely follow high-latitude convection streamlines derived from SuperDARN and satellite observations, although the lower-latitude sunward convecting regions were missed in the

All Supporting Information may be found in the online version of this article.

[1]Bradley Department of Electrical and Computer Engineering, Virginia Tech, Blacksburg, Virginia, USA.
[2]Now at Institute for Geophysics and Extraterrestrial Physics, Technische Universität Braunschweig, Braunschweig, Germany.
[3]Haystack Observatory, Massachusetts Institute of Technology, Westford, Massachusetts, USA.

Corresponding author: E. G. Thomas, Bradley Department of Electrical and Computer Engineering, Virginia Tech, Blacksburg, VA, USA. (egthomas@vt.edu)

2169-9380/13/10.1002/jgra.50116

SuperDARN coverage. *Hosokawa et al*. [2010] investigated the temporal evolution and spatial structure of a TOI driven by a coronal mass ejection (CME), finding that both positive storm effects and a buildup of source plasma in the midlatitude ionosphere are necessary for the formation of a continuous polar TOI.

[5] Results from other studies have suggested that an SED plume will not always give rise to a TOI. *Coster et al*. [2006] identified several storms when SED structures were produced, but no TOI was observed to reach into the dayside cusp region. The strength and/or orientation of the interplanetary magnetic field (IMF) were suggested as possible factors controlling the formation of a TOI from SED.

[6] The goals of this paper are to further understand the mechanisms responsible for the formation of TOI from SEDs and to determine why a TOI does not always occur when an SED is present. It is now possible to make continuous, direct observations of convection electric fields at midlatitudes in the region where this generation of TOI from SED occurs. Recently constructed SuperDARN radars at midlatitudes in North America overlook an increasingly dense network of GPS receivers capable of observing large-scale density structures such as SED and the midlatitude trough [*Coster et al*., 2003; *Coster et al*., 2007; *Basu et al*., 2008]. New analysis tools developed at Virginia Tech allow for side-by-side comparisons of these two datasets on a global scale in a variety of formats. We present an analysis of CME-driven geomagnetic storm activity on 26–27 September 2011 that featured both TOI and SED features.

2. Datasets

2.1. SuperDARN HF Radars

[7] The Super Dual Auroral Radar Network is an international network of HF coherent radars. SuperDARN radars operate continuously to measure line-of-sight (LOS) velocities, backscattered power, and spectral width from decameter-scale plasma irregularities in the ionosphere [*Greenwald et al*., 1985; *Chisham et al*., 2007]. The measured $\mathbf{E} \times \mathbf{B}$ drift velocities of these plasma irregularities are routinely used to derive global electric field maps that describe the large-scale circulation of plasma in the ionosphere [*Ruohoniemi and Baker*, 1998]. The radars are frequency agile over a bandwidth of 8–20 MHz to allow for monitoring of different propagation modes and to follow changing ionospheric conditions. The standard scan mode consists of 16 beams separated in azimuth by 3.3° with sampling in 45 km range gates that begin at a distance of 180 km, creating a field of view (FOV) that extends ~52° in azimuth and several thousand kilometers in range. A full scan typically allows for 1 or 2 min resolution in this mode. Figure 1 shows the coverage available with SuperDARN as of July 2012 in both the northern and southern hemispheres.

[8] In order to better map the expansion of the high-latitude convection pattern during periods of geomagnetic disturbance, the SuperDARN network has been expanding to midlatitudes. The first two North American midlatitude radars were constructed in Virginia at the NASA Wallops Space Flight Facility (2005) and on the grounds of the Virginia Tech Agricultural Research and Extension Center facility near Blackstone (2008). With the support of the NSF Mid-Sized Infrastructure Program, a chain of midlatitude radars is under construction, with twin-radar builds completed in Kansas (2009) and Oregon (2010). These midlatitude radars have provided new opportunities to examine midlatitude ionospheric electrodynamics with unprecedented spatial and temporal coverage [*Oksavik et al*., 2006; *Baker et al*., 2007]. Recently, *Clausen et al*. [2012] examined the time evolution and longitudinal velocity variations of a SAPS feature observed across North America while *Grocott et al*. [2011] and *Kunduri et al*. [2012] studied the magnetospheric dynamics and interhemispheric conjugacy of a SAPS event observed simultaneously in the northern and southern hemispheres.

[9] The velocity measurements from the SuperDARN HF radars can be combined into a global map of ionospheric plasma convection using the technique described by *Ruohoniemi and Baker* [1998] and *Shepherd and Ruohoniemi* [2000]. Figure 2 shows the map obtained for the 19:30–19:32 UT interval on 26 September 2011. The contours of constant electrostatic potential constitute streamlines for *F* region plasma convection. The pattern is predominantly

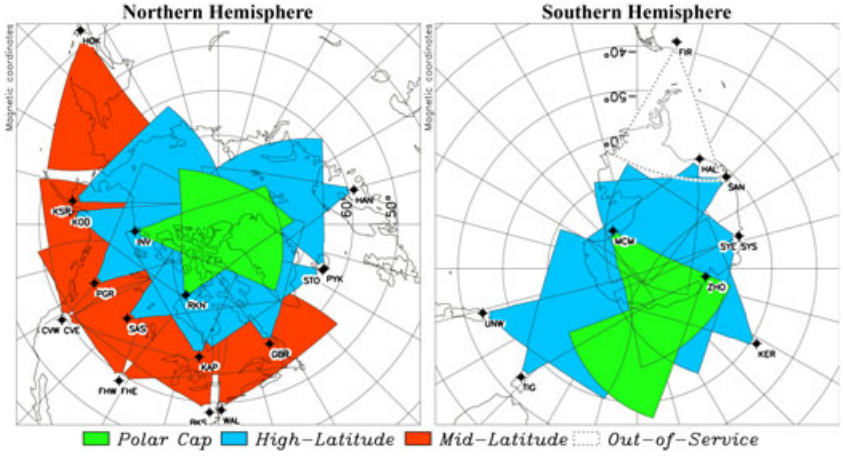

Figure 1. Fields of view of SuperDARN radars in the (left) northern and (right) southern hemispheres as of July 2012. Midlatitude, high-latitude, and polar radar FOVs are shaded red, blue, and green, respectively.

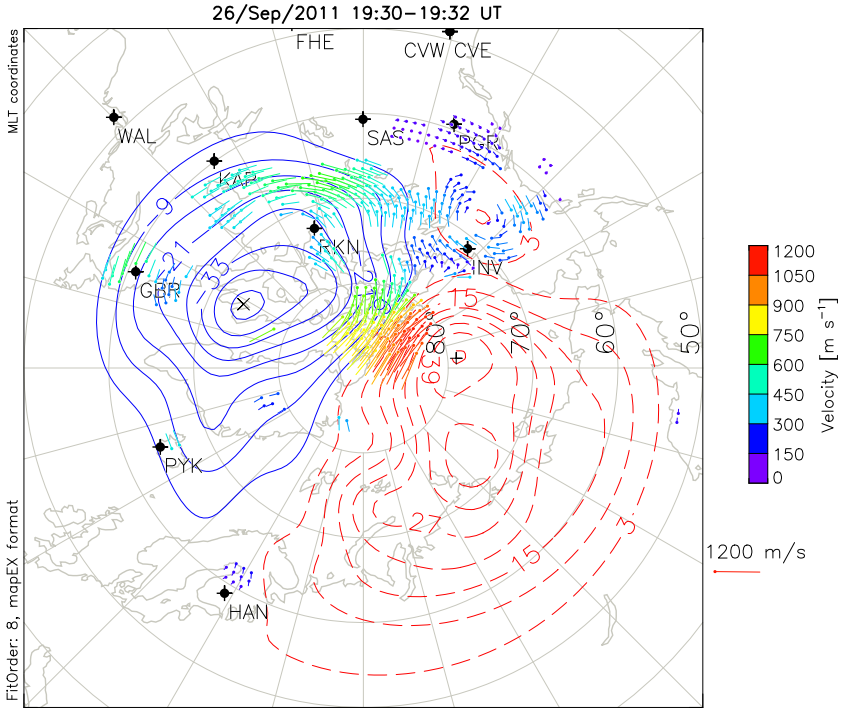

Figure 2. Map of plasma convection obtained for 26 September 2011, 19:30–19:32 UT, using the standard SuperDARN fitting technique as described in the text and plotted in MLT with magnetic noon at the top. The contours indicate lines of constant electrostatic potential; the contour step is 6 kV and solid/dashed contours indicate negative/positive signs on the potential. The positions and three-letter names of the radars contributing to the solution are indicated.

two-cell with a pronounced dayside "throat" feature that can be expected to channel plasma into the polar cap from lower latitudes. Velocity vectors are drawn where velocity data were available from the radars; additional data were provided by a statistical model that is keyed to the prevailing IMF conditions. The coverage by the radars is extensive over North America and provides strong constraints for the fitted pattern, in particular, for the convergence of flows on the dayside that defines the throat. For this study, the convection pattern has been generated at a cadence of 2 min. In addition, we present plots of "raw" LOS velocity data from a subset of the SuperDARN radars that overlook the dayside throat feature. These will serve to show the extent of the areas of HF backscattering as well as the directly measured plasma drift velocities. The occurrence of backscatter for the SuperDARN HF radars indicates the presence of small-scale (~10 m) irregularities in the ionospheric plasma.

2.2. GPS TEC

[10] Maps of TEC are commonly used to depict the highly variable nature of the Earth's ionosphere. Researchers at MIT Haystack Observatory generate maps of vertically integrated TEC from a global network of GPS receivers and offer their data product to the larger scientific community via the Madrigal database [*Rideout and Coster*, 2006]. The TEC measurements of the ionosphere describe the total number of electrons contained in a cylinder of cross-sectional area 1 m^2 that extends vertically above a given point on the Earth and extends all the way through the ionosphere. One TEC unit (TECU) is given as 1×10^{16} electrons/m^2; typical peak dayside values can range from less than 10 TECU on a quiet day to the hundreds of TECU observed during strong geomagnetic storm activity. Measurements are binned into $1^\circ \times 1^\circ$ cells at 5 min resolution. TEC data are processed using the minimum scallop estimation approach described in *Rideout and Coster* [2006] with some modifications. The minimum scalloping method depends on the assumption that when the receiver bias is properly accounted for, on average, there should be no correlation between elevation and vertical TEC.

[11] Figure 3a shows three consecutive 5 min GPS TEC maps from 19:25 to 19:40 UT overlaid on top of one another after mapping to magnetic local time (MLT)/magnetic latitude (MLAT) coordinates. Using a standard spatiotemporal median filtering technique, observations derived at MIT Haystack Observatory from the three intervals are used to generate the single TEC map for 19:30 UT seen in Figure 3b. It is important to note that as a result of the filtering technique, no TEC measurements above 85° Λ are included due to difficulties comparing adjacent cells near the pole. The SuperDARN convection pattern from Figure 2 can be overlaid onto the filtered TEC map, as shown in Figure 4a. This reveals that the dayside TEC enhancements that extend from midlatitudes into the polar cap ($\Lambda > 80^\circ$) are substantially ordered by the pattern of convection streamlines. Regions of plasma entrained by high-speed convection flow are indicated by the close spacing of contour lines rather than the pattern's equatorward extent. Figure 4b offers a view of the spatial distribution of radar backscatter and the LOS velocity measurements that were available from a subset of the SuperDARN radars. The spatial correspondence especially at higher latitudes is suggestive that the TEC

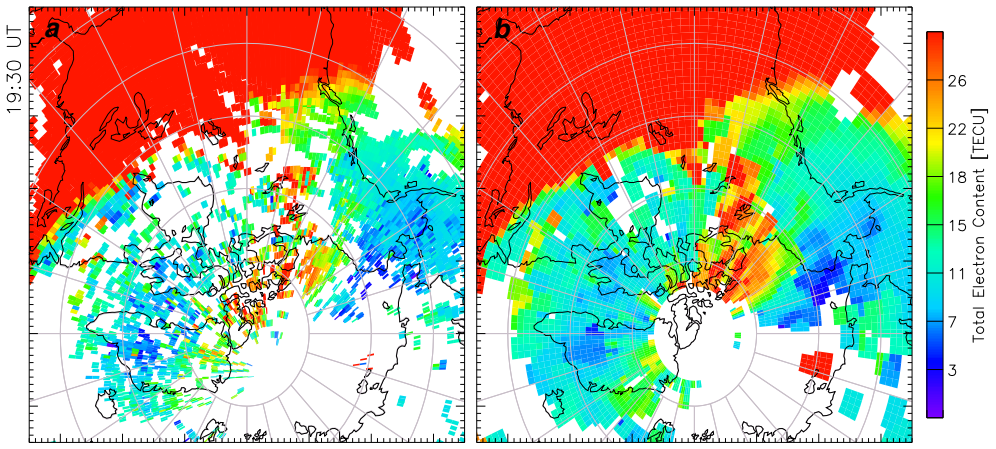

Figure 3. (a) Three 5 min maps of GPS TEC observations overlaid on top of one another from 19:25 to 19:40 UT, after mapping to MLT/MLAT coordinates. (b) Median-filtered GPS TEC data spanning the same interval, centered at 19:30 UT. No TEC data are plotted above $\Lambda = 85°$ due to difficulties in spatial filtering over the polar cap. Figures are plotted with magnetic noon at the top.

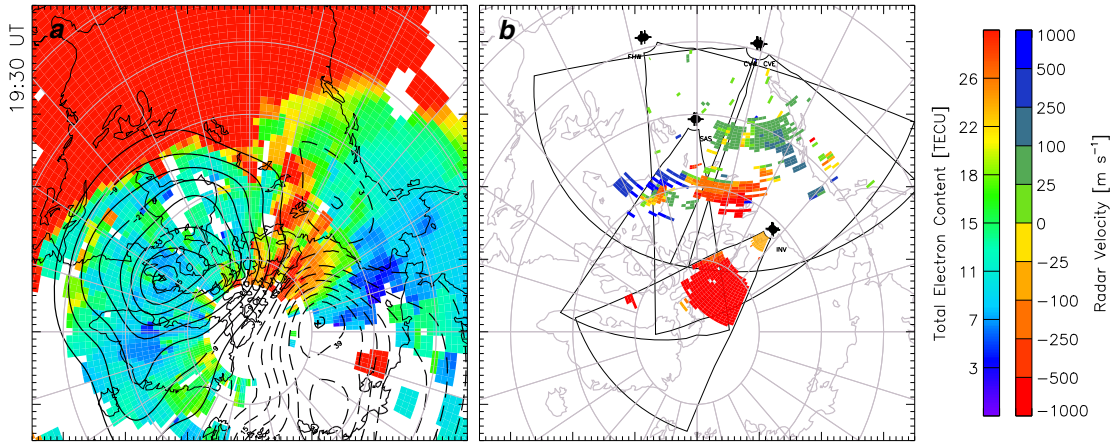

Figure 4. (a) GPS TEC map with SuperDARN convection pattern overlaid and (b) line-of-sight (LOS) velocity measurements from selected SuperDARN radars with fields of view indicated, again plotted with magnetic noon at the top.

enhancement regions were associated with the small-scale irregularities responsible for HF coherent backscatter. A nonlinear color scale has been used for the LOS velocities to better observe variability in the low-velocity flows seen at midlatitudes in addition to the high-velocity motion across the polar cap.

2.3. Online Plotting Tools

[12] The plotting tools applied in this study are available online at the Space@VT SuperDARN website (http://vt.superdarn.org). Using GPS data downloaded from the Madrigal database, users are able to perform spatial/temporal median filtering of the TEC data, turn on and off radar measurements, overlay convection patterns, select from different coordinate systems, and choose the hemisphere to be displayed. Options are also available to plot measurements for a single 5 min period or as an animation over a user-defined interval. Source code and documentation for the use of the plotting tools are freely available on the website.

3. Observations

3.1. Event Overview

[13] In this paper, we examine the formation of a polar TOI from midlatitude SED during a CME-driven geomagnetic storm on 26–27 September 2011. Solar IMF has been demonstrated to strongly affect the features of SEDs and TOIs [*Foster et al.*, 2005; *Hosokawa et al.*, 2010]. Figure 5 shows geomagnetic indices and solar wind parameters for a 16 h period during this event. The arrival of the CME at the Earth's magnetosphere is seen in the top panel at 12:40 UT as an abrupt intensification followed by a steady decline from +50 to –100 nT in the Sym-H index, which is a proxy for the strength of the symmetric part of the ring current.

[14] We have surveyed the timeline of SED and TOI occurrence in the TEC data and determined that a linked SED/TOI event occurred between 18:30 and 19:40 UT and that a second SED period lacked an accompanying TOI in the 20:30–00:30 UT interval. These periods are highlighted in Figure 5 and clearly fall into the storm main phase.

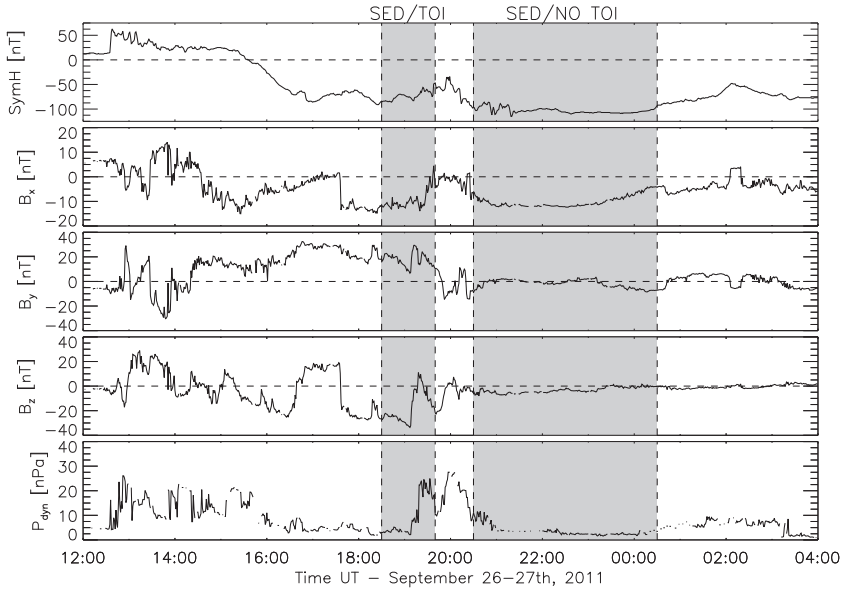

Figure 5. Geomagnetic and solar wind OMNI parameters on 26–27 September 2011: (from top) Sym-H index, OMNI IMF Bx, By, Bz, and dynamic pressure. The first shaded region indicates the interval from 18:30 to 19:40 UT when a TOI formed from midlatitude SED as identified from GPS TEC maps (SED/TOI). The second shaded region indicates a later period from 20:30 to 00:30 UT when no TOI was observed forming from midlatitude SED (SED/NO TOI).

[15] The next three panels in Figure 5 show the IMF Bx, By, and Bz components from the OMNI 2 database [*King and Papitashvili*, 2006]. The interval when a TOI was observed (first shaded region) is characterized by sustained positive IMF By and a strong southward IMF (< –20 nT) until the northward turning at 19:15 UT. Coincident with this northward Bz turning was an increase in solar wind dynamic pressure from nearly zero to 25 nPa (bottom panel). Thirty minutes later at 20:00 UT, a second and final northward Bz turning was also accompanied by a sudden increase in dynamic pressure. After the TOI had subsided and only an SED plume remained (second shaded region), the IMF By and Bz components remained fairly constant and low in magnitude. The positive By and southward Bz components of the IMF from 17:30 to 19:20 UT meet the conditions described by *Hosokawa et al.* [2010] for the formation of a continuous polar TOI. As we shall see, the large transitions in Bz during the early part of the storm controlled the evolution of the SED and emergence of TOI.

3.2. Formation of TOI

[16] Following the southward turning of the IMF at 17:37 UT on 26 September 2011 (Figure 5), an SED plume began to form over eastern North America. Figure 6 shows the

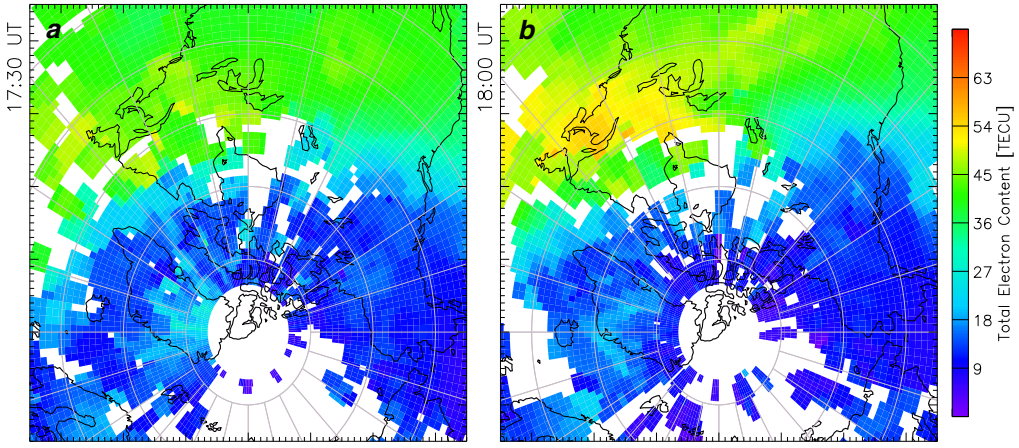

Figure 6. GPS TEC maps showing the development of an SED plume over North America at (a) 17:30 UT and (b) 18:00 UT on 26 September 2011. The color scale has been increased from Figures 3 and 4 to highlight the region of enhanced TEC below 60° Λ corresponding to the SED plume in Figure 6b. Figures are plotted with magnetic noon at the top.

TEC distribution in the Northern Hemisphere before and just after the southward turning. At 17:30 UT, the midlatitude plasma densities appeared fairly uniform in magnitude on the dayside (Figure 6a). Thirty minutes later at 18:00 UT, a new region of enhanced TEC corresponding to an SED plume was emerging at middle latitudes in the afternoon sector (Figure 6b). Note that we have increased the TEC color scale from that applied in Figures 3 and 4 in order to show the SED feature more prominently. Examination of driftmeter data from the Defense Meteorological Satellite Program spacecraft suggests the presence of SAPS disturbance electric fields during this period, although there is a local time difference of almost 4 h between the satellite crossings on the dusk flank and the plume of enhanced TEC over North America.

[17] A continuous polar TOI was observed to have formed from the midlatitude SED in GPS TEC measurements from 18:30 to 19:40 UT. Figure 7 shows the time evolution of the TOI, ionospheric convection, and HF backscatter patches

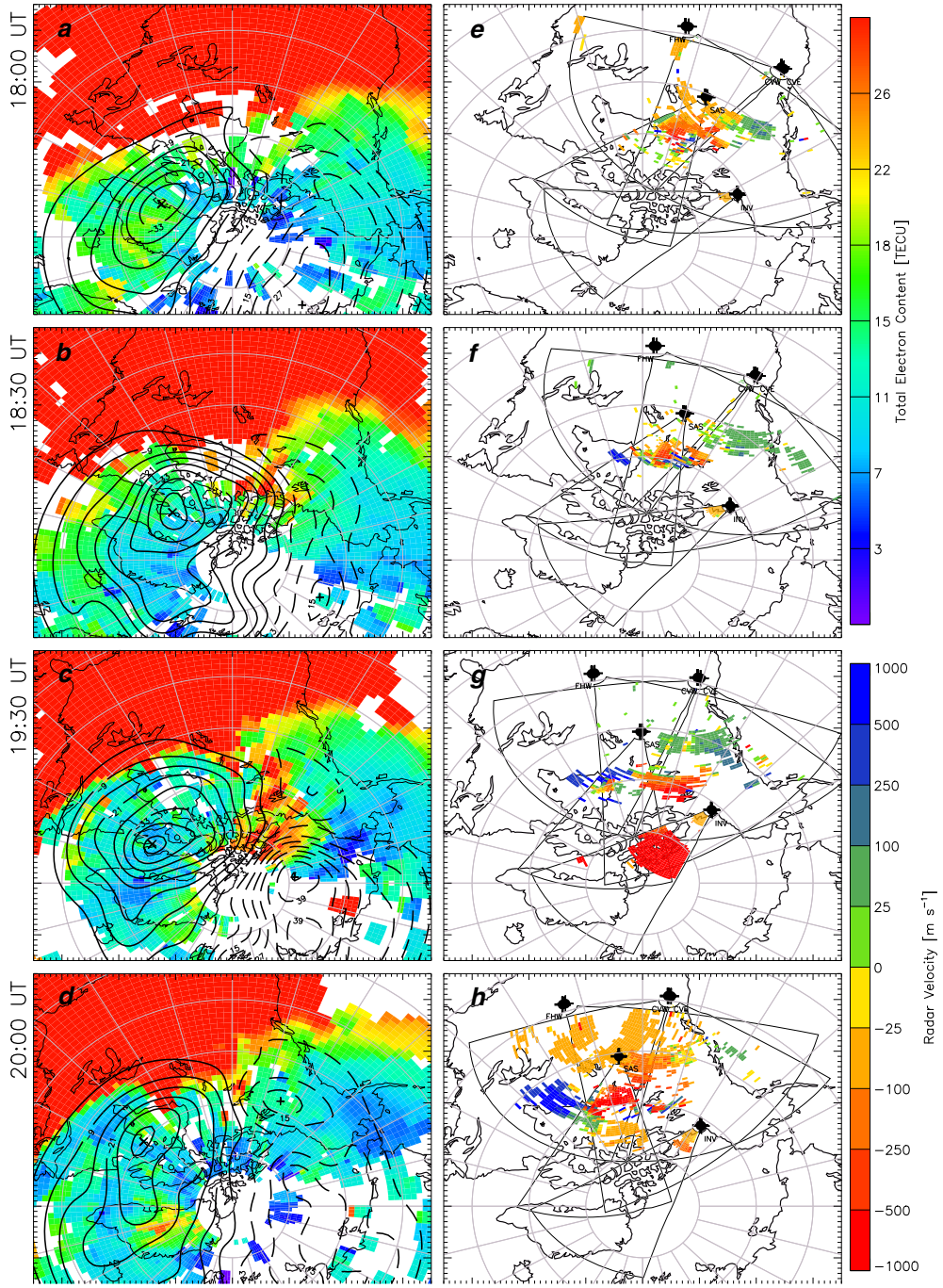

Figure 7. (a–d) GPS TEC maps depicting evolution of a polar tongue of ionization (TOI) with SuperDARN convection patterns overlaid. (e–h) SuperDARN LOS velocity measurements from ionospheric scatter for selected radars. Figures are plotted in MLT with magnetic noon at the top for times 18:00, 18:30, 19:30, and 20:00 UT.

as seen by GPS TEC and SuperDARN. A channel of enhanced TEC is seen progressing poleward from a midlatitude SED feature by 18:30 UT and entering the polar cap by 19:30 UT. Similar to the results presented by *Foster et al*. [2005], the channel of enhanced TEC closely follows the streamlines of convection independently derived from the global network of SuperDARN radars. Sustained positive IMF By lasting until 19:50 UT was responsible for the clockwise rotation of the global convection pattern, bringing the dusk cell onto the dayside. When combined with the strongly southward IMF, this allows for the enhanced dusk convection cell to transport dense midlatitude ionospheric plasma into the throat feature as seen in Figure 7b.

[18] The plasma within the TOI was convected across the pole at speeds in excess of 1 km/s. The continuous TOI persisted until just after 19:30 UT, when the base of the TOI detached from its source region at middle latitudes. Changes in the IMF conditions altered the convection pattern such that more of the plasma flow in the throat was associated with the dawn cell, which lacked a connection

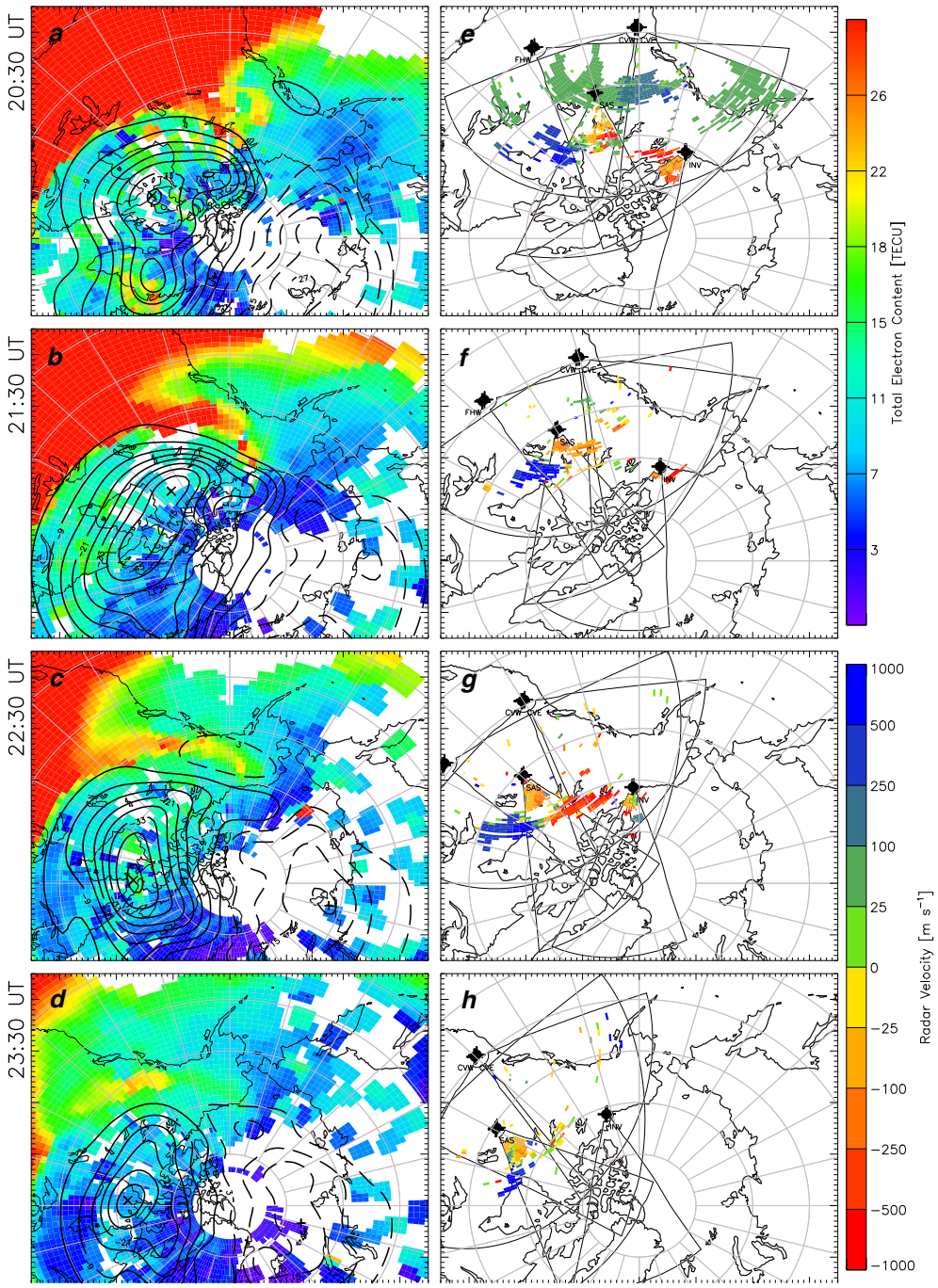

Figure 8. In the same format as that of Figure 7: (a–d) GPS TEC maps depicting evolution of "fossil" storm enhanced density (SED), and (e–h) radar velocity measurements for times 20:30, 21:30, 22:30, and 23:30 UT.

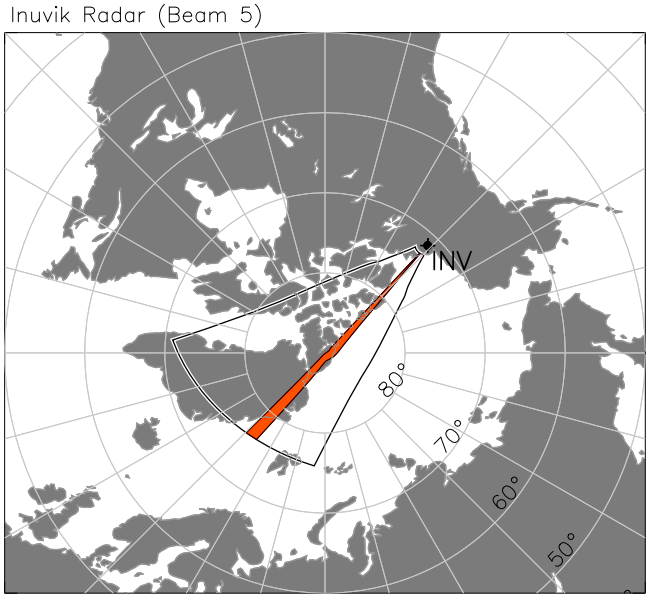

Figure 9. Field of view of Inuvik radar, with beam 5 highlighted, plotted with magnetic noon at the top of the figure for 19:30 UT. This beam looks into the polar cap and is aligned with the throat of the TOI feature described in the text.

to a high-density reservoir of plasma. The SuperDARN velocity plots on the right-hand side of Figure 7 show regions of HF backscatter due to small-scale irregularities and the accompanying LOS plasma velocity. Although many factors influence the occurrence of HF backscatter, there are indications that the TOI is a source of backscatter [*Hosokawa et al.*, 2009]. In particular, by 19:30 UT, an irregularity backscatter patch had formed in the polar cap that was spatially coincident with the extension of the TOI, suggesting small-scale irregularity formation. Figure 7d indicates that by 20:00 UT, the large continuous patch of plasma had broken up into smaller patches that have begun to exit the polar cap and become entrained in the dusk convection cell. A movie of GPS TEC maps showing the evolution of SED/TOI activity is available in the online auxiliary materials.

3.3. Storm Enhanced Density

[19] A plume of enhanced TEC was observed some time after the disappearance of the TOI (Figures 8a–8d). One endpoint of the SED plume was attached to the dense source plasma at middle latitudes in the afternoon sector while the other remained fixed in MLAT/MLT near the dayside cusp. As the midlatitude region of enhanced TEC corotated with the Earth away from noon, the plume elongated in MLT at a near-constant latitude and lasted until approximately 00:30 UT on 27 September 2011. The backscatter observed by the SuperDARN radars remained poleward of this region throughout its duration (Figures 8e–8h). This implies that, unlike the earlier TOI formed from an SED, this plume was not the seat of active irregularity formation. While IMF Bz was still negative during this period (Figure 5), it was greatly reduced in magnitude from the earlier SED/TOI interval and IMF By was near zero. (Although the Bx component was substantial, its impact on convection during equinoctial periods is thought to be minimal.) The spacing of the contours in the low-latitude region widened during the interval from

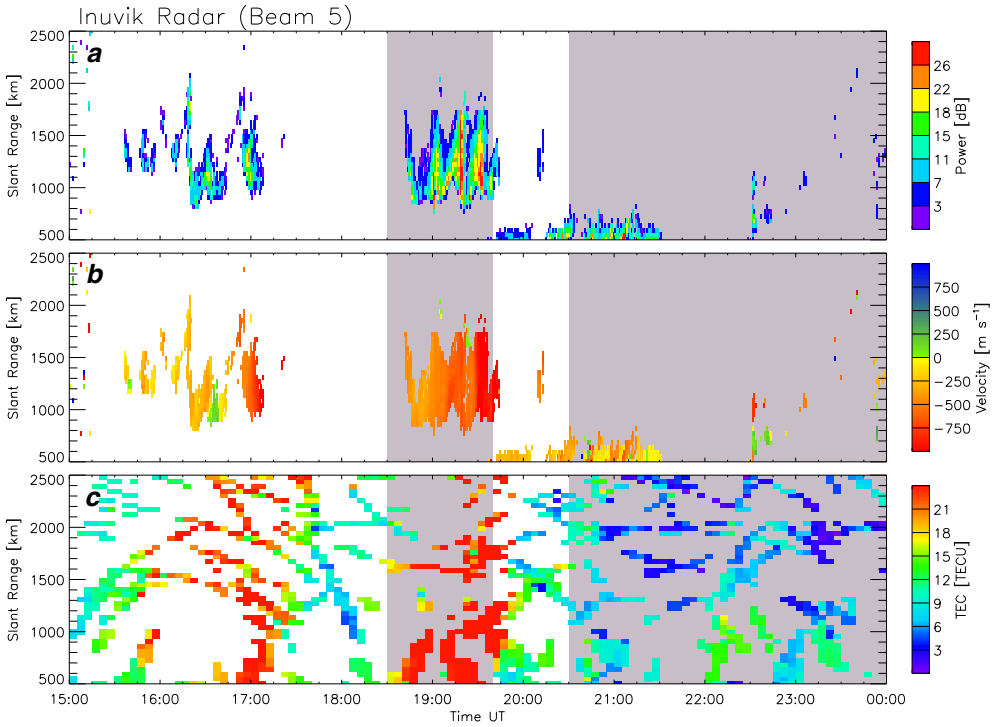

Figure 10. (a) The backscattered power and (b) LOS Doppler velocity data from beam 5 of the polar Inuvik radar in range-time-intensity format. (c) GPS TEC data closest to each range cell along the same beam. In the same manner as in Figure 5, the two intervals of SED activity as observed from GPS TEC maps are shaded.

18:30 to 20:00 UT (Figures 7b–7d) indicating a reduction in the flows associated with the northward turning of the IMF. By the time the convection strengthened again due to the southward turning of the IMF at 20:30 UT (Figure 8b), it is clear that the convection did not extend to low enough latitudes for the SED plume to be entrained to flow into the polar cap. This plume was consequently unproductive in terms of TOI and small-scale irregularity formation, and persisted rather as a "fossil" feature within the plasma distribution.

[20] We examined GPS TEC and SuperDARN data along a selected radar beam to gain further insight into the degree of spatial coincidence of the density enhancements and backscatter from small-scale irregularities. The Inuvik radar is situated at a very high latitude ($\Lambda = 71.5°$) and looks deep into the polar cap as shown in Figure 9. Figure 10 shows backscattered power, LOS Doppler velocity, and nearest GPS TEC data along beam 5 of the Inuvik SuperDARN radar as a function of slant range (distance travelled by a transmitted signal through the ionosphere to a backscattering irregularity). The two intervals of SED activity previously indicated in Figure 5 are again highlighted in each of the panels. The plot of backscattered power indicates that a sequence of poleward propagating HF backscatter patches was observed in the latter part of the first interval. These were associated with very high velocities away from the radar (antisunward), at the same time that the region of enhanced TEC passed through the radar FOV over the polar cap. Thus, the TOI was productive of small-scale irregularities within patchy-like features. No sign of the later "fossil" SED seen in Figure 8c was observed in either the radar or TEC polar cap measurements, indicating that the high-TEC plasma was no longer being convected to high latitudes. (An earlier TOI at 16:30 UT can be seen entering the radar FOV in Figure 10c, although the lower velocities and shorter duration observed by the radar suggest a weaker event.)

4. Discussion

[21] We have presented observations of the formation of a polar TOI during a geomagnetic storm on 26–27 September 2011 using GPS TEC and SuperDARN measurements. Early in the event, the high-latitude convection electric fields expanded equatorward to middle latitudes, encountering a region of enhanced plasma and entraining the flow of dense *F* region plasma through the dayside cusp and across the polar cap at velocities in excess of 1400 m/s. This scenario has been postulated previously by *Foster et al*. [2005] and *Hosokawa et al*. [2010]. Here, for the first time, simultaneous measurements of GPS TEC and SuperDARN ionospheric convection at midlatitudes have been available to confirm the equatorward expansion of the high-latitude convection electric fields into the dense source region and the poleward retreat of the convection pattern which strands the resulting fossil SED at subauroral latitudes. It is also shown that the TEC enhancements that map out the TOI are associated with small-scale irregularities responsible for HF backscatter. By the end of the second interval, the distribution of dayside ionospheric plasma changed such that the region of enhanced TEC was confined to the dusk sector at middle latitudes over North America. This temporal variation in the distribution of midlatitude source plasma would require longer transport times to the cusp, and thus, newly convected plasma would be depleted before reaching the cusp inflow region.

[22] The fossil SED observed from 20:30 to 00:30 UT has many features similar to the event described by *Coster et al*. [2006], which did not form a TOI despite the plume of enhanced TEC reaching the dayside cusp region. For the 26–27 September 2011 event, during the inactive SED period, IMF conditions returned to a quiet state with both the By and Bz components nearly zero (Figure 5). No ionospheric backscatter was observed by SuperDARN radars within the region of enhanced TEC that persisted, suggesting the disappearance of the drivers responsible for small-scale irregularity formation. This inactive persistence is very similar to the fossil ionospheric trough described by *Evans et al*. [1983], whereby an ionospheric perturbation formed by an active storm process will persist in the absence of daylight as it corotates through the night sector at a near-constant latitude. This phenomenon has also been discussed in relation to subauroral ion drifts (now known as SAPS) and stable auroral red arcs by *Anderson et al*. [1991] and *Foster et al*. [1994]. The later SED plume (Figure 8) is in effect a remnant of the earlier activity and akin to a "fossil" SED feature. By contrast, the earlier SED encountered strong electric fields and produced a TOI.

[23] We conclude our discussion by summarizing the SED/TOI activity through the two intervals in terms of magnetic reconnection. When the IMF Bz component turned strongly southward, enhanced dayside reconnection results in plasma that was previously on closed field lines at lower latitudes being subsequently on open field lines. This leads to the excitation of convection electric fields as the newly open flux evolves over the magnetopause, thus drawing plasma from the closed field line region (where the SED is located) into the polar cap (producing the TOI). When IMF Bz experiences a northward turning, dayside reconnection stalls, and there is no longer a mechanism allowing plasma to move from the closed to the open field line regime [*Cowley and Lockwood*, 1996]. Hence, the SED plume stagnates as a fossil feature, and no TOI is produced.

5. Summary

[24] In this paper, we have examined the relationship of convection electric fields to the formation of a polar cap TOI from midlatitude plumes of SED. Observations from the geomagnetic storm on 26–27 September 2011 were presented for two cases of potential TOI formation from an SED. During an hours-long period of dynamic geomagnetic activity, a channel of high-density *F* region plasma was transported from the dayside midlatitude ionosphere and into the polar cap by enhanced convection electric fields extending to middle latitudes ($\Lambda = 60°$). The TEC enhancements that mapped out the TOI were associated with HF backscatter, indicating that the TOI is the seat of active formation of small-scale irregularities. After the solar wind IMF conditions quieted and the dayside convection electric fields retreated to higher latitudes ($\Lambda \geq 70°$), an SED plume was observed extending to, but not entering, the dayside cusp region. This high-TEC feature persisted at a near-constant latitude for several hours and elongated in MLT as one endpoint remained fixed near the cusp while the other

corotated with the dense source region over North America. No ionospheric scatter from the SuperDARN radars was observed within this remnant SED region. For this fossil feature, the source mechanism (enhanced electric fields) previously drawing the plasma from midlatitudes and into the polar cap was no longer locally active. Thus, we have demonstrated the controlling role exercised by the convection electric field in generating a TOI from midlatitude SED.

[25] **Acknowledgments.** The authors from Virginia Tech thank the National Science Foundation for support under grants AGS-0946900 and AGS-0838219. The authors from MIT Haystack also thank the National Science Foundation for support under grant ATM-0856093. EGT acknowledges support provided by the Virginia Space Grant Consortium under a graduate research fellowship. LBNC acknowledges funding from the Deutsches Zentrum fuer Luft- and Raumfahrt under grant 50OC1102 and 50OC1001. Sym-H indices were obtained from the World Data Center in Kyoto. The OMNI data were obtained from the GSFC/SPDF OMNIWeb interface at http://omniweb.gsfc.nasa.gov. The TEC data were downloaded through the Madrigal database at Haystack Observatory. The authors acknowledge the use of SuperDARN data. SuperDARN is a collection of radars funded by national scientific funding agencies of Australia, Canada, China, France, Japan, South Africa, United Kingdom, and the United States of America.

References

Anderson, P. C., R. A. Heelis, and W. B. Hanson (1991), The ionospheric signatures of rapid subauroral ion drifts, *J. Geophys. Res.*, *96*(A4), 5785–5792.

Baker, J. B. H., R. A. Greenwald, J. M. Ruohoniemi, K. Oksavik, J. W. Gjerloev, L. J. Paxton, and M. R. Hairston (2007), Observations of ionospheric convection from the Wallops SuperDARN radar at middle latitudes, *J. Geophys. Res.*, *112*(A1), 1303, doi:10.1029/2006JA011982.

Basu, Su., S. Basu, J. J. Makela, E. MacKenzie, P. Doherty, J. W. Wright, F. Rich, M. J. Keskinen, R. E. Sheehan, and A. J. Coster (2008), Large magnetic storm-induced nighttime ionospheric flows at midlatitudes and their impacts on GPS-based navigation systems, *J. Geophys. Res.*, *113*(A3), A00A06, doi:10.1029/2008JA013076.

Chisham, G., M. Lester, S. E. Milan, M. P. Freeman, W. A. Bristow, A. Grocott, K. A. McWilliams, J. M. Ruohoniemi, T. K. Yeoman, and P. L. Dyson (2007), A decade of the Super Dual Auroral Radar Network (SuperDARN): Scientific achievements, new techniques and future directions, *Surv. Geophys.*, *28*(1), 33–109.

Clausen, L. B. N., et al. (2012), Large-scale observations of a subauroral polarization stream by midlatitude SuperDARN radars: Instantaneous longitudinal velocity variations, *J. Geophys. Res.*, *117*(A5), A05306, doi:10.1029/2011JA017232.

Coster, A. J., J. C. Foster, and P. J. Erickson (2003), Monitoring the ionosphere with GPS: Space weather, *GPS World*, *14*(5), 42–49.

Coster, A. J., M. Colerico, J. C. Foster, and J. M. Ruohoniemi (2006), Observations of the tongue of ionization with GPS TEC and SuperDARN, *Haystack Observatory, Westford, MA*.

Coster, A. J., M. J. Colerico, J. C. Foster, W. Rideout, and F. Rich (2007), Longitude sector comparisons of storm enhanced density, *Geophys. Res. Lett.*, *34*(18), L18, 105, doi:10.1029/2007GL030682.

Cowley, S. W. H., and M. Lockwood (1996), Time-dependent flows in the coupled solar wind-magnetosphere-ionosphere system, *Adv. Space Res.*, *18*(8), 141–150.

Evans, J. V., J. M. Holt, W. L. Oliver, and R. H. Wand (1983), The fossil theory of nighttime high latitude F region troughs, *J. Geophys. Res.*, *88*(A10), 7769–7782.

Foster, J. C. (1993), Storm time plasma transport at middle and high latitudes, *J. Geophys. Res.*, *98*(A2), 1675–1689.

Foster, J. C., M. J. Buonsanto, M. Mendillo, D. Nottingham, F. J. Rich, and W. Denig (1994), Coordinated stable red arc observations: Relationship to plasma convection, *J. Geophys. Res.*, *99*(A6), 11,429–11,439.

Foster, J. C., and W. J. Burke (2002), SAPS: A new categorization for sub-auroral electric fields, *EOS Trans. AGU*, *83*(36), 393.

Foster, J. C., and H. B. Vo (2002), Average characteristics and activity dependence of the subauroral polarization stream, *J. Geophys. Res.*, *107*(A12), 1475.

Foster, J. C., A. J. Coster, P. J. Erickson, F. J. Rich, and B. R. Sandel (2004), Stormtime observations of the flux of plasmaspheric ions to the dayside cusp/magnetopause, *Geophys. Res. Lett.*, *31*, L08809, doi:10.1029/2004GL020082.

Foster, J. C., et al. (2005), Multiradar observations of the polar tongue of ionization, *J. Geophys. Res.*, *110*(A9), A09S31, doi:10.1029/2004JA010928.

Greenwald, R. A., K. B. Baker, R. A. Hutchins, and C. Hanuise (1985), An HF phased-array radar for studying small-scale structure in the high-latitude ionosphere, *Radio Sci.*, *20*(1), 63–79.

Grocott, A., S. E. Milan, J. B. H. Baker, M. P. Freeman, M. Lester, and T. K. Yeoman (2011), Dynamic subauroral ionospheric electric fields observed by the Falkland Islands radar during the course of a geomagnetic storm, *J. Geophys. Res.*, *116*(A11), A11, 202.

Heppner, J. P., and N. C. Maynard (1987), Empirical high-latitude electric field models, *J. Geophys. Res.*, *92*(A5), 4467–4489.

Hosokawa, K., K. Shiokawa, Y. Otsuka, T. Ogawa, J.-P. St-Maurice, G. J. Sofko, and D. A. Andre (2009), Relationship between polar cap patches and field-aligned irregularities as observed with an all-sky airglow imager at Resolute Bay and the PolarDARN radar at Rankin Inlet, *J. Geophys. Res.*, *114*(A3), A03306, doi:10.1029/2008JA013707.

Hosokawa, K., T. Tsugawa, K. Shiokawa, Y. Otsuka, N. Nishitani, T. Ogawa, and M. R. Hairston (2010), Dynamic temporal evolution of polar cap tongue of ionization during magnetic storm, *J. Geophys. Res.*, *115*(A12), A12, 333, doi:10.1029/2010JA015848.

King, J., and N. Papitashvili (2006), One min and 5-min solar wind data sets at the Eart's bow shock nose, *NASA Goddard Space Flight Cent., Greenbelt, MD*.

Knudsen, W. C. (1974), Magnetospheric convection and the high-latitude F2 ionosphere, *J. Geophys. Res.*, *79*(7), 1046–1055.

Kunduri, B. S. R., J. B. H. Baker, J. M. Ruohoniemi, L. B. N. Clausen, A. Grocott, E. G. Thomas, M. P. Freeman, and E. R. Talaat (2012), An examination of inter-hemispheric conjugacy in a subauroral polarization stream, *J. Geophys. Res.*, *117*(A8), A08, 225, doi:10.1029/2012JA017784.

Oksavik, K., R. A. Greenwald, J. M. Ruohoniemi, M. R. Hairston, L. J. Paxton, J. B. H. Baker, J. W. Gjerloev, and R. J. Barnes (2006), First observations of the temporal/spatial variation of the sub-auroral polarization stream from the SuperDARN Wallops HF radar, *Geophys. Res. Lett.*, *33*, L12, 104.

Rideout, W., and A. Coster (2006), Automated GPS processing for global total electron content data, *GPS Solutions*, *10*(3), 219–228.

Ruohoniemi, J. M., and K. B. Baker (1998), Large-scale imaging of high-latitude convection with Super Dual Auroral Radar Network HF radar observations, *J. Geophys. Res.*, *103*(A9), 20,797–20.

Ruohoniemi, J. M., and R. A. Greenwald (1996), Statistical patterns of high-latitude convection obtained from Goose Bay HF radar observations, *J. Geophys. Res.*, *101*(A10), 21,743–21.

Sato, T. (1959), Morphology of ionospheric F2 disturbances in the polar regions: A linkage between polar patches and plasmaspheric drainage plumes, *Rep. Ionos. Res. Space Res. Jpn.*, *13*, 91.

Sato, T., and G. F. Rourke (1964), F-region enhancements in the Antarctic, *J. Geophys. Res.*, *69*(21), 4591–4607.

Shepherd, S. G., and J. M. Ruohoniemi (2000), Electrostatic potential patterns in the high-latitude ionosphere constrained by SuperDARN measurements, *J. Geophys. Res.*, *105*(A10), 23,005–23.